

PERFORMANCE OF K-SVD ALGORITHM IN DIGITAL OPTICAL COHERENCE TOMOGRAPHY

RANDRIANARISON Nomenjanahary Tsirilala¹, RANDRIAMITANTSOA Paul Auguste²,
RAMAFIARISONA Malalatiiana Hajaso³

¹PhD student, TASI, ED-STII, Antananarivo, Madagascar

²Thesis director and Laboratory Manager, TASI, ED-STII, Antananarivo, Madagascar

³Thesis co-director, TASI, ED-STII, Antananarivo, Madagascar

ABSTRACT

Optical Coherence Tomography (OCT) is a non-invasive imaging technique for micron-scale biological media with the most notable application in the field of ophthalmology. An expansion of the use of the OCT in question is proposed in this article by inserting a dictionary learning algorithm which is none other than the K-SVD. The objective of this article is therefore the improvement by different aspects of the OCT's performance thanks to the K-SVD algorithm. To do this, we have integrated the K-SVD algorithm in the OCT giving so many solutions to the previous problems given the simulations that follow illustrating the performance of this invention

Keywords: *compression, tomography, K-SVD algorithm, optical coherence.*

1. INTRODUCTION

The temperature is the physical quantity very indispensable in the fields of productions. And most of the In the world of optical imaging, optical coherence tomography is a world in its own right. This imaging technique is based on low coherence light interferometry, developed in the early 1990s, and continues to develop, diversify and specialize, constantly finding new areas of application. It is within this framework of imaging technology, still in full swing, that our article consisting of the demonstration of the "Performance of the K-SVD algorithm in optical coherence tomography" is integrated. After having explained the compression principle, we will report the K-SVD algorithm, then the OCT technique, then the evaluation parameters of the compression performance. At the end, we do some simulations that demonstrate the evaluation of the performance of this technique.

2. PRINCIPALE OF COMPRESSION

We detail through this paragraph the main ideas and fundamental principles leading to different compression methods. The methods of compression vary according to the types of images (natural, medical, satellite, etc.) and the targeted applications (internet, storage, etc.) besides the requirements in terms of quality [1] [2]. The importance of this compression remains the concentration of the energy on few coefficients, so as to create large ranges of zeros after quantification. Compression reduces the number of data to be transmitted. For some signals, it also makes it possible to eliminate existing redundancies in order to reduce the amount of information necessary for their representations. There are two main compression chains [3]

2.1. The lossless compression chain (reversible):

The values of the compressed image are not dependent on any changes to the values of the original image (for example, for medical applications: no diagnostic error can be tolerated). The advantage of this type of chain is to have a reconstructed and identical image. However, its disadvantage lies in the low compression rate that can be achieved. Indeed, this one is limited by the entropy of the source.

Lossless methods can be used directly in a compression chain. However, some of them are often used after the quantization phase of a lossy compression chain, during the transmission or storage of the indexes. We can distinguish [4]:

- Predictive methods:

These exploit the spatial redundancy that exists between the current value and the previous or next values.

- Entropic coders

They try to get as close as possible to the entropy of the sequence of values to be coded, by assigning a number of bits as small as possible to the most probable values and vice versa. Huffman coding and arithmetic coding are the main entropic coders used in the field of image compression.

2.2. The compression chain with loss (not-reversible):

During the quantization phase, changes are made to the values of the image. The advantage of this type of approach is that it is possible to achieve significant compression rates, but at the expense of the quality of the reconstructed image. However, the majority of consumer applications have turned to this type of compression (digital camera, natural images, medical images, transmission of images on different networks, image storage, etc.). Fig -1 shows the main steps of a lossy compression chain [4].



Fig- 1: The three classic steps of image

Lossy image compression methods constitute the majority of research work, especially during the quantization step. We can distinguish:

- Scalar Quantization (QS) based methods:

They consist of treating the values (of pixels or coefficients) individually. Different types of Scalar Quantification exist, and are still used.

- My methods based on Vector Quantification (QV)

At the same time, they treat a group of pixels or coefficients, called vectors. They theoretically allow to be always more efficient than methods based on Scalar Quantification.

2.3. The different stages of compression.

Current medical image compression methods follow the 3 standard image compression steps. Most of these begin with a reorganization of the content of the image, in order to separate the important components of the components containing little information by using the K-SVD. This task is fulfilled by a mathematical transformation. After this step, it follows quantization which irreversibly degrades the signal, then the coding takes the relay by which a bit stream is produced [5] [4].

- Step One: Data Transformation

The purpose of data transformation in a compression scheme is twofold. Indeed, in addition to reorganizing the information, it must represent the important components of a signal with the least possible elements: this is called a hollow representation of the signal or compact the energy.




The purpose of reducing redundancy is to reduce correlations between pixels. It focuses the variations (energies) of the image on some samples and distributes almost uniformly the correlated pixels.

- Second step: Quantification

In a compression phenomenon, the quantization step is the step that irreversibly degrades the signal. It is, however, of utmost importance in reducing the bit rate. By quantization, we mean an operation that transforms a continuous signal into a discrete signal using a set called dictionary. This transition from continuous to discrete can be done sample by sample.

Despite the fact that quantization makes it possible to gain significant compression ratio, it is a stage where information is lost. Since the quantization operation consists in removing certain information, it is thus a lossy operation that will give a loss of precision, which is irreversible. The lower the quantization accuracy, the more you gain a compression ratio, but you also lose more information [6].

Table-1: Image Quantify at Different Levels

 <p>a) Medical image with the size of 29.3 KB</p>	 <p>b) Image Quantize at 10 Bpp making the size of 5.45 Ko</p>	 <p>c) Image quantize at 90 bps making the size of 31.2 Ko</p>
---	--	--

- Third step: coding:

There are two main families of encoders: entropic encoders and range encoders. They are used in a compression chain directly on the starting image and they are also used in the last step of the compression chain to exploit the redundancies present at the output of the quantization [7].

Fig-2 shows the diagram of the functionality of the compression, storage or transmission and decompression of an image.

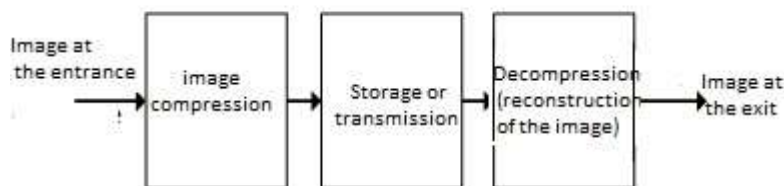


Fig -2: Compression and decompression of an image for storage or transmission.

Seeing all the compression techniques, the explanation of the K-SVD algorithm follows one another.

3. K-SVD ALGORITHM

3.1. Definition

K-SVD is a useful algorithm for solving the parsimonious dictionary learning problem and consists of an alternate optimization [8] [9] [10].

The parsimonious dictionary learning is written by the following formula:

$$\min_{D,X} \{\|Y - DX\|_F^2\} \text{ tel que } \forall i \|x_i\|_0 \leq T_0 \tag{3.01}$$

Where $\|x_i\|_0$ is the norm l_0 of the vector x_i , that is to say, the number of its non-zero components.

Iteratively solve a partial problem in X, fixed D. This step is called parsimonious coding step (where "sparse coding" on English) in which one seeks to solve:

$$\min_x \{\|Y - DX\|_F^2\} \text{ tel que} \tag{3.02}$$

$$\forall i \in \{1; N\} \|x_i\|_0 \leq T$$

3.2. Implementation of the K-SVD algorithm

The problem of equation (3.02) is convex.

However, the combinatory linked to the use of the l_0 standard make the resolution of the image impeccable. These methods require approximating the norm l_0 to the norm l_1 . For this modified formulation, the problem of optimization, resolutions will be solved.

It is then proposed to tackle the complex problem presented in equation (3.02) (norm l_0) by using an approximated algorithm to solve it. The solution will be derived from a method based on Orthogonal Matching Pursuit (OMP). The required functions will be provided.

The second step is to optimize D and fix X of the K-SVD. We therefore seek to solve:

$$f(D) = \|Y - DX\|_F^2 = \left\| Y - \sum_{j=1}^K d_j x_T^j \right\|_F^2 \tag{3.04}$$

$$= \left\| (Y - \sum_{j=1}^{K-1} d_j x_T^j) - d_K x_T^K \right\|_F^2 = \|E_K - d_K x_T^K\|_F^2 \tag{3.05}$$

Each product $d_j x_T^j$ is a matrix of size $n \times N$ The term E_k in equation (3.05) is the data reconstruction error made from the $K-1$ elements of the dictionary $\{D_j\}_{j=1}^{K-1}$.

Since we suppose that these elements are fixed, we try to minimize $f(D_k)$. It is possible to minimize by least squares, but we want to ensure that the updated solution always allows parsimonious decomposition. To ensure this property, we will define :

$$W_k = \{i | 1 \leq i \leq N, x_T^k(i) \neq 0\} \tag{3.06}$$

With W_k represents the set of indices (for the examples $Y = \{y_i\}$) which use the atom d_k (that is to say those for which $x_T^k(i) \neq 0$)

- Method used for optimization

To optimize d_k , we then use the following method:

One restricts the matrix E_k to form E_k^R by considering only the columns corresponding to W_k If one notes Ω_k my matrix of size $N \times W_k$ corresponding to copy N times the line vector W_k , we have:

$$E_k^R = E_k \Omega_k \text{ et } x_R^k = x_T^k \Omega_k \tag{3.07}$$

- Solution

Thanks to equation (3.07), the following formulation (3.08) becomes easier to handle:

$$\|E_k - d_k x_T^k\|_F^2 \tag{3.08}$$

Both with respect to d_k and x_R^k , ensuring that the support x_T^k (that is, w_k , those not null) remains unchanged. To determine $\min_{d_k, x_T^k} \|E_k - d_k x_T^k\|_F^2$, we use a Singular Value Decomposition SVD of $E_k^R = U\Delta V^T$.

The solution for d_k and x_R^k is then the following:

- d_k is the first column of U
- x_R^k is the first column of V multiplied by $\Delta(1, 1)$.

Here is a figure that gives an overview of the k-SVD algorithm

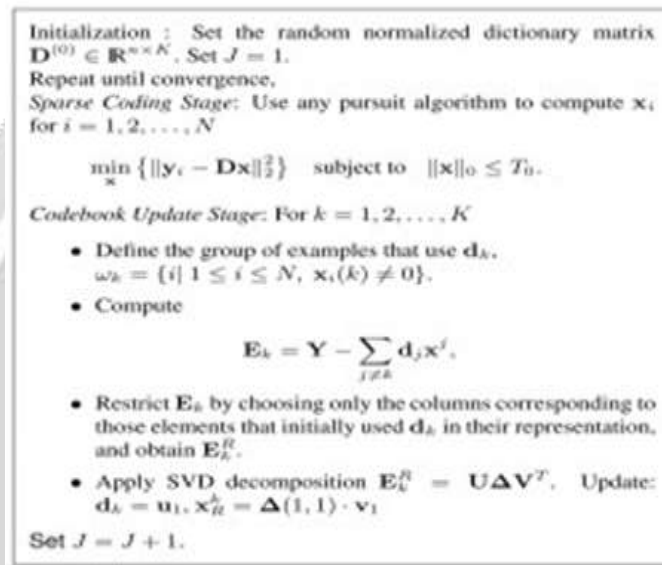


Fig-3: K-SVD algorithm

After studying the K-SVD algorithm, we will begin the examination of what is called OCT.

4. THEORY OF OPTICAL COHERENCE TOMOGRAPHY

4.1. General principles of OCT

OCT measures photon amplitude and flight time using the highly sensitive technique of low coherence interferometry or white light interferometry [11]. It is the phenomenon that is at the origin of the beautiful iridescent colors that we see on thin layers such as soap bubbles or petrol stains. It was applied for the first time in biology in 1988 for measuring the length of the eye. Here is the figure that shows this principle.

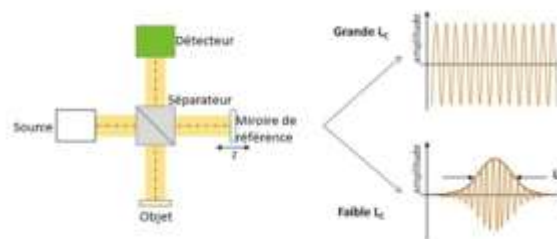


Fig-4: Michelson interferometer: principle of interferometry and coherence length

That system presented in Fig-4 is also called Michelson interferometer. The light from the source is divided in amplitude in two arms by a separating surface which is called in this "separator" figure: the object arm

comprising the sample, and the reference arm with a known reflecting surface. The flight time of the light coming from the object sample, of amplitude E_{ob} , is measured by recombining it with the reference beam, of amplitude E_r , whose flight time (the length of the arm) is known. The field that arrives on the detector is the sum of the two fields in amplitude $E_r + E_{ob}$. The measured intensity is:

$$I \sim |E_r|^2 + |E_{ob}|^2 + 2E_r E_{ob} \cos\left(\frac{2\pi}{\lambda} \delta\right) \tag{4.01}$$

Where δ is the difference in the interferometer (in μm). That is, the optical path difference between the two arms. The resulting intensity is the sum of the intensities reference $|E_r|^2$ and object $|E_{ob}|^2$ and a crossword of interference $2E_r E_{ob}$.

4.2. Modulation of the interference term

The term interference is modulated by the coherence: interference is detected with the reference arm only when the path is the same to a coherence length close, that is to say $|\delta| \leq L_c$. The temporal coherence length L_c is a characteristic of the light source; it defines the maximum operating difference on which the interference is visible [4]. The interferences are therefore only detected in an area of the object called the coherence volume, which is actually a thickness plane $L_c / 2n$ with n the index of the medium. For an ideal Gaussian profile spectrum, L_c depends on the spectrum of the source according to the formula [11].

$$L_c = \frac{2 \ln 2}{\pi} \frac{\lambda_0^2}{\Delta \lambda} \tag{4.02}$$

The wider the spectrum (large $\Delta \lambda$), the lower the coherence length. Indeed, in a wide spectrum, the interference systems due to each wavelength are superimposed and scrambled, because they each have a distinct phase difference $2\pi / \lambda \delta$. In terms of order of magnitude, sunlight, as seen by our eye, has a coherence length of $0.5\mu\text{m}$. The light of a sophisticated Ti: Sapphire femtosecond laser (spectrum width 150nm to 200nm centered around 800nm) has a coherence length around $2\mu\text{m}$.

However, note that this does not mean, beyond the length of coherence, interference does not cease to exist, they are always present but only less contrasting

4.3. The different configurations of OCT

There are different configurations of OCT according to the method of acquisition and processing of the interferometric signal. They differ according to the techniques used at each OCT [12].

- Conventional OCT

The tomographic image (XZ) is acquired in the temporal space by scanning the reference mirror (Z) and transverse scanning the beam (X). The acronym for this OCT is TD-OCT (Time Domain Optical Coherence Tomography). [11]. [12]. So it's a temporal optical coherence tomography. This OCT allows the correlation of the wave reflected and / or backscattered by the object with a reference wave. The waves coming from the two arms of the interferometer, separated and then recombined by the splitter plate, interfere if the difference in operation is less than the temporal coherence length of the light source. A detector, usually a photodiode, acquires this interferometric signal. To access the structural information of the sample in depth (type A scan), the reference mirror is translated during acquisition by the detector shown in Fig-5.

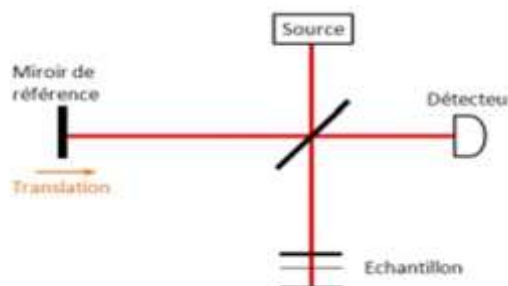


Fig -5: Schematization of the principle of temporal optical coherence tomography.

In the following, we will describe the principle of frequency and full field OCT configurations, as well as their comparative advantages.

- Frequency optical coherence tomography

The tomographic image (XZ) is acquired in the frequency space by scanning the wavelength or acquisition by a spectrometer (Z) and transverse scanning of the beam (X). The acronym for this OCT is FD-OCT, which is called frequency-domain coherence tomography (or Fourier Domain Coherence Tomography). This concept, proposed by Fetcher and AI in 1995, is based on the principle that depth information is also encoded in the modulation frequencies of the interference signal spectrum [12] [17]. The axial profile is therefore no longer recorded as a function of time but as a function of the frequency or the wavelength and therefore no longer requires scanning of the reference mirror, which allows a considerable gain in acquisition time by report to TD-OCT.

Two solutions are possible to experimentally record this axial profile as a function of the wavelength. D-OCT in the spectral domain and D-OCT spectral scanning.

4.4. Integration of the image signal processing system into the OCT using the K-SVD algorithm.

- Introduction

This section discusses the integration of the D-OCT component technologies described in a complete imaging system that will be seen in Fig-6. This includes both hardware considerations such as optimal interferometer topologies and scanning synchronization dynamics, as well as software integrations such as acquisition, transformation, display, and enhancement of images. using the K-SVD algorithm. A limited discussion on first generation slow scanning systems is included when illustration; However, most of the discussion focuses on the the-art state of OCT systems that acquire images in near real time.

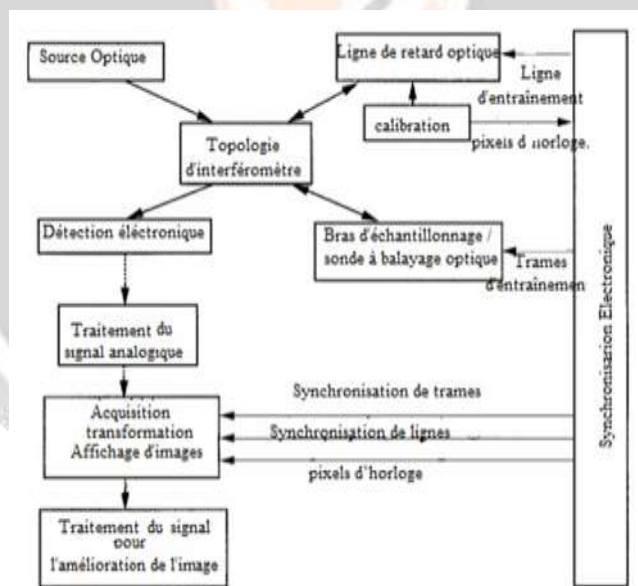


Fig-6: Block diagram of the D-OCT system components and synchronization requirements.

In this figure, the thick lines represent the optical signals, the dashed lines represent the electronic signals and the thin lines represent the synchronization signals.

- Determination of the block that integrates the K-SVD algorithm

In this section, we show the adaptation of the synoptic diagram of the components of the OCT systems with the k-SVD algorithm. This algorithm utilizes principal component analysis in the transformation block. This transformation is then followed by an adaptive uniform scalar quantization whose pitch varies according to the dynamics of the block. The encoding operation converts each coefficient of the quantized transformed matrix into a binary word. The reconstruction of the image proceeds in the opposite direction of the compression.

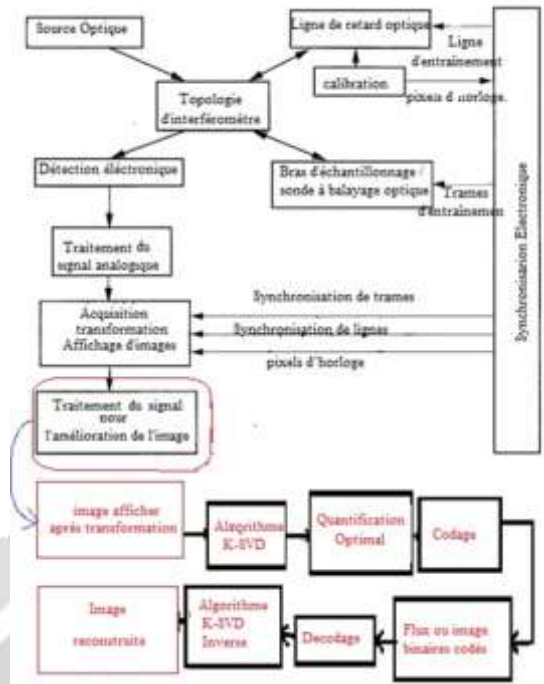


Fig-7: Synoptic diagram of OCT K-SVD.

5. THE PERFORMANCE CRITERIA OF HIS METHODS.

The purpose of image compression, whether lossless or lossy, is to obtain the best image quality after compression and decompression with a given compression ratio and bits per pixel.

In order to satisfy the requirements of users as most men only observe the final images, it is also necessary to use mathematical methods of image quality measurements before saying whether the technique is the right one or not. Subsequently, the evaluation of the quality of an image regardless of its type, tomographic among others, will be more realistic. Quantities (mathematical methods) are usually used to appreciate the performance of a storage and even compression technique based on the combination of "K-SVD Algorithm with D-OCT".

The image storage and compression performance parameters described in this article are: compression ratio (Cr), compression rate, Peak Signal Noise Ratio (PSNR), and Structural Similarity (SSIM).

5.1. Compression ratio (Cr)

The compression ratio (Cr) in English is a measure to determine the performance of a data compression technique, whether it is lossless or lossy. It describes the relationship between the size of the original image and the size of the compressed image.

This compression ratio is defined by the following equation [20] [21]:

$$T = \frac{D_{out}}{D_{in}} \tag{5.01}$$

Or:

- T Represents the compression ratio;
- D_{in} Express the size of the raw data;
- D_{out} Express the size of the compressed data.

To express the compression ratio as a percentage, we apply the inverse operation of equation (5.01) while multiplying the result by 100 [21]:

$$T_{\%} = \frac{D_{out}}{D_{in}} \times 100 \quad (5.02)$$

$$T_{\%} = T \times 100$$

Or:

$T_{\%}$ Represents the compression ratio as a percentage.

From Equation (5.01), a value of 0.5 means that the size of the data occupies 50% (applying the formula (5.02)) of its original size after compression. A value greater than 1 means that the volume of data output is greater than the original (a negative compression).

Another expression of the compression ratio in equation (5.03) is also used to express the percentage of space saved after compression.

$$T'_{\%} = (1 - T) \times 100 \quad (5.03)$$

From this expression (5.03), a value of 50 means that the size of the data compressed at the output occupies 50% of the original data size, and the compression has saved 50% of space [22].

5.2. Bitrate compression rates per pixel

Apart from the compression ratio used to evaluate image compression performance, a similar notion to compression rates is also used: the bit-by-pixel amount (b / pixel or bpp).

This is the average number of bits needed, to compress a pixel of the image especially in image. This quantity is given by the following formula:

$$BPP = \frac{B_{img}}{P_{img}} \quad (5.04)$$

$$BPP = \frac{B_{img}}{L_{img} \times H_{img}}$$

Or:

- B_{img} Represents the bit size of the image
- P_{img} represents the number of pixels of the image which is equal to the width of the image
- L_{im} multiplied by the height of the image H_{img}
- Its unit of measure is the Bpp or B / pixel

This BPP amount, after the compression of the image, must be compared with the Bpp of the image before compression.

5.3. Peak Signal Noise Ratio (PSNR)

PSNR is a quantity to measure the quality of the reconstructed image after decompression. The calculation of the PSNR is defined by the following equation:

$$PSNR(x, y) = 20 \log_{10} \frac{\max(X_i)}{EQM(x, y)} \quad (5.05)$$

With $\max(X_i)$ represents the maximum value that each pixel of the image can take. For an 8bit grayscale image for example, it has a value of 255. For color images, it is the luminance that is used.

5.4. The structural similarity index or Structural Similarity (SSIM)

The SSIM was introduced by Zhou Wang, Alan Conrad Bovid, Hamid Rahim Sheikh, and Eero P. Simoncelli in 2004 [19]. It is a calculation metric used to measure the similarity between two images. It was developed based

on the findings that conventional image quality measurement techniques such as PSNR are unconvincing compared to human visual perception.

The difference, compared to the PSNR measurement techniques, is that the latter estimate the perceived errors of each pixel of the image (compared to the original) whereas the SSIM considers the degradation of the image as perceived (observable) changes. at the structural information level of the image.

The usual measurement techniques are based on error sensitivity. These techniques do not consider the structure of the image.

Thus, the researchers brought a new mathematical approach to find a new way to include the image structure similarities especially the medical image as the tomographic image to compare the original image and the degraded image.

The SSIM between two images x and y of the same size $N \times N$ (or of a window of size $N \times N$) is obtained by the following equation

$$SSIM(x, y) = \frac{(2\mu_x\mu_y + C_1)(2\sigma_{xy} + C_2)}{(\mu_x^2 + \mu_y^2 + C_1)(\sigma_x^2 + \sigma_y^2 + C_2)} \quad (5.06)$$

Or :

- x , and y are the two windows to compare,
- μ_x is the average of x
- μ_y is the average of y
- σ_x^2 represents the variance of x , and σ_y^2 that of y
- σ_{xy} represents the covariance of x and y
- $C_1 = (k_1L)^2$, $C_2 = (k_2L)^2$ represent two variables to stabilize the division by a low denominator,
- $L = 2^{BPP} - 1$, (BPP bit-by-pixel sampling)
- and $k_1 = 0.01$, $k_2 = 0.03$ by default.

6. APPLICATION OF THIS TECHNIQUE IN A TOMOGRAPHIC IMAGE EXAMPLE

This technique finds its application especially in the medical field. For these reasons, it will be more interesting to carry out examples, which, like frequent cases, use the OCT.

6.1. Optical coherence tomography in ophthalmology

Ophthalmology remains the preferred field of application for optical coherence tomography. The main reasons for this craze are:

- The high transmission of the ocular medium which allows to reach depths of penetration of the order of millimeters,
- The interferometric sensitivity and micrometric spatial resolution of the OCT technique, which resolve most of the structures of interest of the eye,
- The independence of the axial resolution with the numerical aperture of the probe beam, which makes it possible to image the structures of the eye, in particular the retina, with a high axial resolution although the numerical aperture is very limited by the size from the pupil of the eye.

For these reasons, the use of the K-SVD algorithm is very important. OCT's commercial instruments have become commonplace, as are traditional techniques in an ophthalmic examination (including Cirrus OCT devices such as Zeiss Stratus OCT and Thorlabs SS-OCT). The instrument marketed by Carl Zeiss Meditec, the Cirrus HD-OCT (FD-OCT device), makes it possible to perform in vivo tomographic slices with a resolution of approximately $5 \mu\text{m}$ (Fig -8) and an acquisition speed of 25,000. One-scan per second. This very high acquisition rate makes it easy to perform in vivo clinical examinations. However, the resolution must be substantially improved in order to detect certain pathological diseases affecting the intrathecal structures, unsolved with $5 \mu\text{m}$.



Fig-8: Cirrus HD-OCT Commercial Instrument by Carl Zeiss Meditec.

In the laboratory, a number of applications have been made in the field of ophthalmology, in particular for the diagnosis of pathologies. Fig -9 and table -2 respectively show high-resolution OCT tomographic slices of an ex vivo rat cornea in axial and transverse reconstruction.

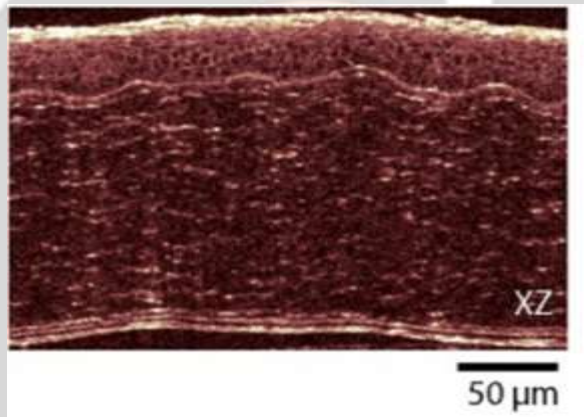
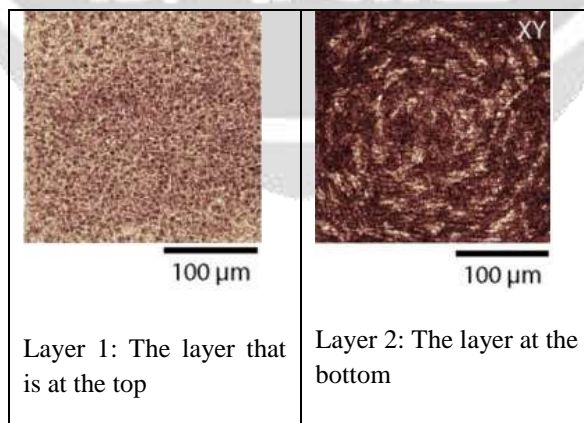


Fig-9: Tomographic images obtained by OCT in axial reconstruction of an ex vivo rat cornea

Table -2: Tomographic images obtained by OCT in transverse reconstruction of an ex vivo rat cornea

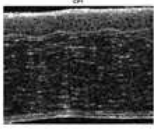




6.2. Application of the k-SVD algorithm in the tomographic image

- Vector approach

Vector approach that is to say the transformation is applied to a matrix using the K-SVD algorithm. The projection on the factorial axes with the percentages of inertia for each principal axis is given by the following table.

Table -3: The three main components of the OCT image of an ex vivo rat cornea.

Principle component 1	Principle component 2	Principle component 3
		
Inertie = 90,2%	Inertie = 8,9%	Inertie = 0,9%

The totality of the image energy is divided into three main components, the first of which contains most of it. This distribution depends on the size of the bulk partitioning performed on the image.

So a good choice of the number of main components and the block size is a decisive parameter in the compression. It must be done judiciously taking into account the law of distribution of the energy in the image and its contents even if experimental values between 80% and 90% can be practically chosen.

- Marginal approach

The efficiency of a transformation can also be judged by its power of reconstruction, that is to say its capacity more or less great to reconstruct the original image according to the energy distribution. One way to measure this capability is to use metrics such as compression ratio, P.S.N.R and S.S.I.M which are objective indicators of degradation of the reconstructed image. In practice, threshold values are chosen for the two quantities, from which the acceptable degradation is considered. Frequently used ranges are 30 dB to 40 dB for P.S.N.R and 0.8 to 0.9 for S.S.I.M.

- Simulation at compression ratio levels

For this assessment, after setting the quantization levels. We obtain the following figure:

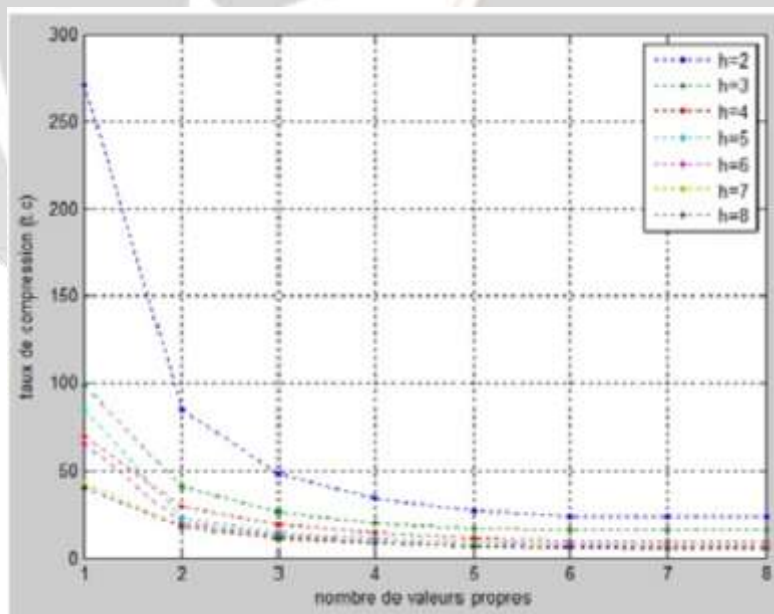


Fig 10: Compression rate as a function of the number of eigenvalues for fixed h.

It can be said that the compression ratio is a measure of the performance of a data compression technique such as the tomographic image. It describes the relationship between the size of the original image and the size of the compressed image.

- Simulation at PSNR level

The variations of P.S.N.R as a function of block size and as a function of eigenvalue for fixed h are illustrated by the following figures in the case of the tomographic image of a cornea of a rat.

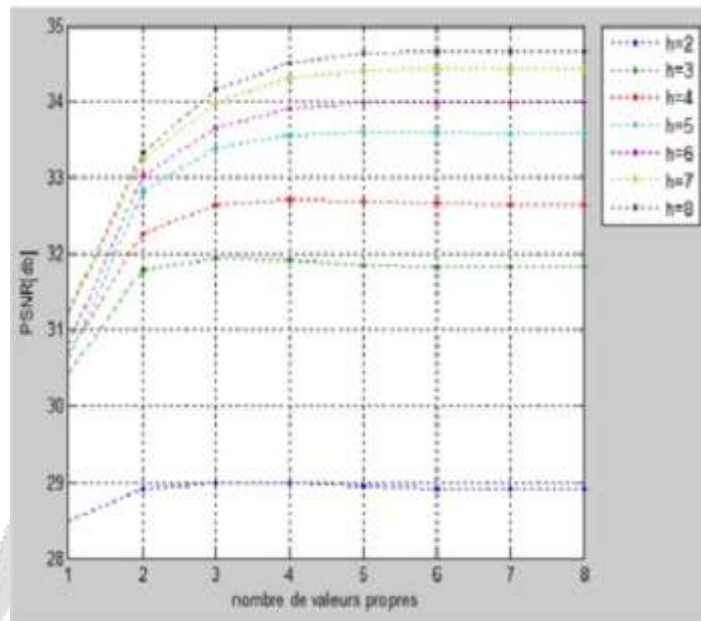


Fig -11: PSNR according to the number of proper value. for fixed h.

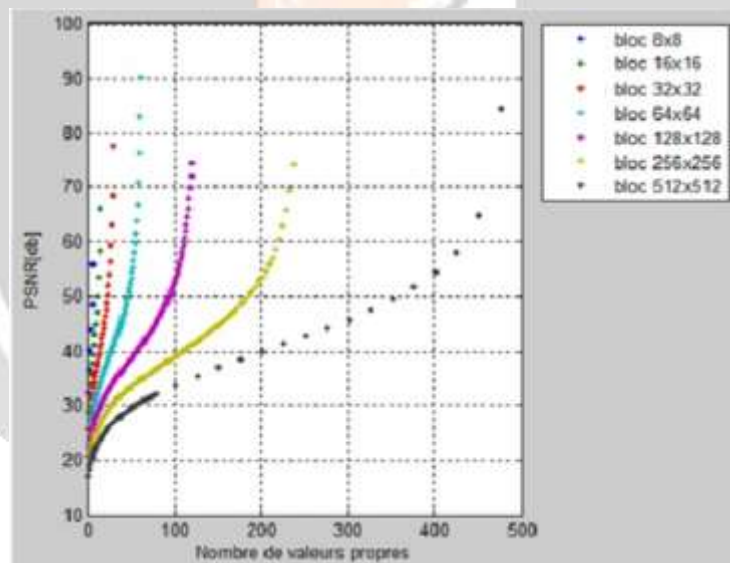


Fig -12: Variation of PSNR according to the number of proper value.

The figure shows that P.S.N.R varies much more rapidly when the size of the block decreases and this rapid variation is observed in the vicinity of the extremal values that can be taken as number of eigenvalues. Among other things, for a 8x8 block image, the total number of eigenvalues is 8. The value of the PSNR is already in the range [30 40] dB when less than 50% of the eigenvalues are taken.

- Simulation at the level of the SSIM

For this mathematical method, we will also see the variations according to the block size and as a function of eigenvalue for fixed h. The following figures show the results.

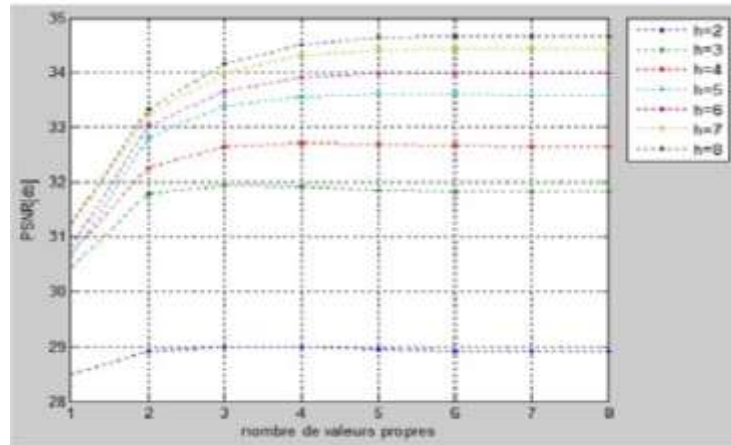


Fig -13: SSIM as a function of the number of proper value for h fixed.

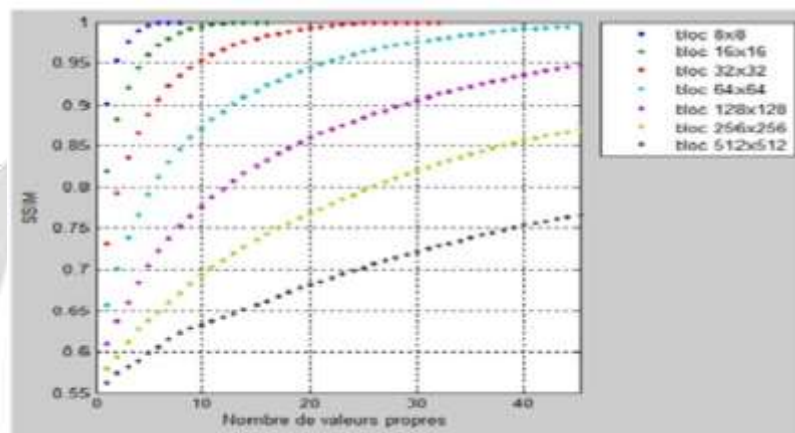


Fig-14: Variation of the SSIM according to the number of proper value

Contrary to what had happened for the RN, the SSIM tends to flatten when the number of eigenvalues to keep approaches the maximum values. This phenomenon comes from the fact that the eigenvalues are ordered in the decreasing direction and that the cumulative inertia percentages are almost constant in the vicinity of the maximum values

7. CONCLUSIONS

The study in this paper examines the performance of the K-SVD algorithm in the OCT technique. On different images of tomographic acquisition, the criterion of comparison is of course the quality of the image at the reconstruction for the different values of the number of projections. By relying on the PSNR values obtained and the visual results, the K-SVD algorithm gives a better performance for a large number of projections or displays. Can we do the same project for other non-medical images?

8. REFERENCES

- [1] M.H. Ramafiharisona, « traitement des signaux numérique », cours DEA à l'école Supérieure Polytechnique d'Antananarivo, Département Télécommunication, 2012-2013.
- [2] M.A.Rakotomalala, « traitement d'image numérique avec ondelette », cours DEA, à l'école Supérieure Polytechnique d'Antananarivo, Département télécommunication, 2012-2013.
- [3] O.Mohand, « Compression d'images hyperspectrales par la transformée en ondelettes 3D », Université Mouloud Mammeri; Tizi-Ouzou, Faculté de Genie Electrique et de l'Informatique; Département d'électronique, 29 Septembre 2011.

- [4] M. Ouahiouane, « Compression d'image hyperspectrales par la transformée en ondelettes 3D », Mémoire de magister en électrique, 29 Novembre 2011.
- [5] Y. Gaudeau, J.M. Moureaux, « Un schéma de compression avec perte efficace pour les images médicaux volumiques », Faculté de Sciences et Technique, Article (SPIHT3D), 2006.
- [6] S. Mallat, « A Wavelet tour Of Signal Processing (2nd Ed.) », 1999.
- [7] Y. Gagou, « cours de traitement d'image », Université de Picardie Jules Venne, 2007-2008.
- [8] S. Lesage, « Apprentissage de dictionnaires structurés pour la modélisation parcimonieuse des signaux multicanaux », Université Rennes 1, 2007.
- [9] M. Aharon; M. Elad; A. Bruckstein « Learning Multiscale Sparse representations for Image and Video Restoration », Multiscale Model Simul, Vol 7, N°1, pp214-241, 2008
- [10] J. Mairal; G. Sapiro; M. Elad; « design of dictionaries for sparse representation », Israel Institute of Technology, 2007.
- [11] A. Latrive, « Tomographie de cohérence optique plein champ pour l'endoscopie : microscopie in situ et in vivo des tissus biologiques », Université Pierre et Marie Curie - Paris VI, 2012.
- [12] B. E. Bouma; G. J. Teaney, « *Optical Coherence* », 2002.
- [13] B. Recur, « *Précision et qualité en reconstruction tomographique: Algorithmes et Applications* », Ecole Doctorale de Mathématiques et Informatique, 29 Novembre 2010
- [14] M. Servières, « *reconstruction tomographique Mojette* », Ecole Doctorale Sciences et Technologie de L'Information et Des Matériaux, 07 Décembre 2005
- [15] D. Saechet, « *Tomographie par cohérence optique plein champ linéaire et non linéaire* », Université Paris Sud - Paris XI, 2010.
- [16] C. Nabil, M. Zoubeida, S. Amina, « *la méthode descente de gradient pour la reconstruction tomographique des images 2D à rayon X* », Journal of Advanced eSearch and Technology, ISSN :2352 - 9989
- [17] M. S. M Yussof, R. Sulaiman, K. Shafinah, R. Fatihah, « *image reconstruction of computed tomography using fan-beam technique* », Int. J. Eng, CS&Tech, 2012, v0105, 06 – 11, ISSN: 2277 - 9337
- [18] D. T. Nguyen, « *développement d'algorithmes de reconstruction tomographique pour l'analyse PIXE d'échantillons biologiques* », Nuclear Theory, Université Sciences et Technologies – Bordeaux I, Université des Sciences Naturelles – Hanoi, 2008
- [19] Z-E, Baarir, A. Oaoui, « *Etude de la transformée en ondelettes dans la compression d'images fixes* », Laboratoire de recherche LESIA, Département d'Electronique, Université Mohamed Khider, Juin 2004
- [20] Y. Gaudeau, J.M. Moureaux, « Un schéma de compression avec perte efficace pour les images médicaux volumiques », Faculté de Sciences et Technique, Article (SPIHT3D), 2006.
- [21] . Ouahiouane, « Compression d'image hyperspectrales par la transformée en ondelettes 3D », Mémoire de magister en électrique, 29 Novembre 2011.
- [22] J.Mille ; R. Boné ; P. Makris ; H. Cardot, « Surface active pour la segmentation d'image 3D, comparaison de méthode d'évaluation », Université François Rabelouis de Tours Laboratoire Informatique (E.A2101